REMOTE SENSING OF THE HOSSACK ROAD PROJECT - WAIKITE AREA, TAUPO VOLCANIC ZONE, NEW ZEALAND

E.B.Herras

PNOC Energy Development Corporation, Merritt Road, Ft. Bonifacio, 1201 Makati City, Philippines

ABSTRACT

*The **Waikite area is located in the Maroa Volcanic Center of the Taupo Volcanic Zone in North Island, New Zealand. The conventional method of aerial photograph interpretation was used in conjunction with digital topographic data analysis through shaded relief maps, to determine the geological structures of the area. The Waikite area is dominated by five main fracture sets oriented : a) 040°- 050°± 10° b) 320°- 330°± 10° c) 000" - 010° d) 090°- 100°± 10" and e) 060°- 070". The Waikite thermal area falls along the intersection of northeast and northwest trending lineaments which supports earlier workers' findings. The prevailing fault pattern indicates structural deformation by simple parallel wrenching along the major northeast trending faults. Compressive forces are associated with the oblique subduction of the Pacific Plate beneath the North Island.***

1.0 INTRODUCTION

Surface thermal activity is intimately associated with the presence of young active normal faults. The presence of these faults provides fracture permeability, which allows upwelling thermal fluids to discharge. In any geothermal exploration program, mapping of geological features is highly important since it gives a general understanding of the hydrology of an area (P.Browne, 1998). Modern, efficient and fast methods of geological mapping include LANDSAT and SPOT imagery and other forms of satellite data. However, this requires the use of large resources and complex processing facilities (Lueder, 1959). The conventional method of using vertical aerial photographs prior to field investigation still is a reliable and an economic way of accomplishing structural mapping.

This study aims to make a detailed geological and structural map of the Waikite area with the use of the conventional vertical aerial photographs and with a more advanced but cheap method, called digital topographic data. The delineated geological structures from these methods are compared with existing geological and geothermal information and an interpretation of the mapped data is presented. The data acquired fiom this study may be of use in future exploration and development plans of the area.

2.0 THE STUDY AREA

The Waikite Valley is located in the central eastern part of the North Island of New Zealand and is about 300 kilometers southeast of Auckland City (Fig. 1). It lies within the Maroa Volcanic Center of the Taupo Volcanic Zone (TVZ). TVZ is a zone of young eruptive centers and associated geothermal systems extending from Ruapehu to White Island. In general, the TVZ denotes a NNE-SSW trending zone of Late Pliocene to Quaternary arc volcanism fiom Ohakune and White Island to the Kermadec Ridge (Wilson et al., 1995).

The Waikite area is mantled by pyroclastic flows and air fall deposits of rhyolitic composition possibly all originating fiom the Maroa Volcanic center. The surface rock units exposed in the area were mapped and described by Grindley (1960) and their distribution is shown in Fig. 2.

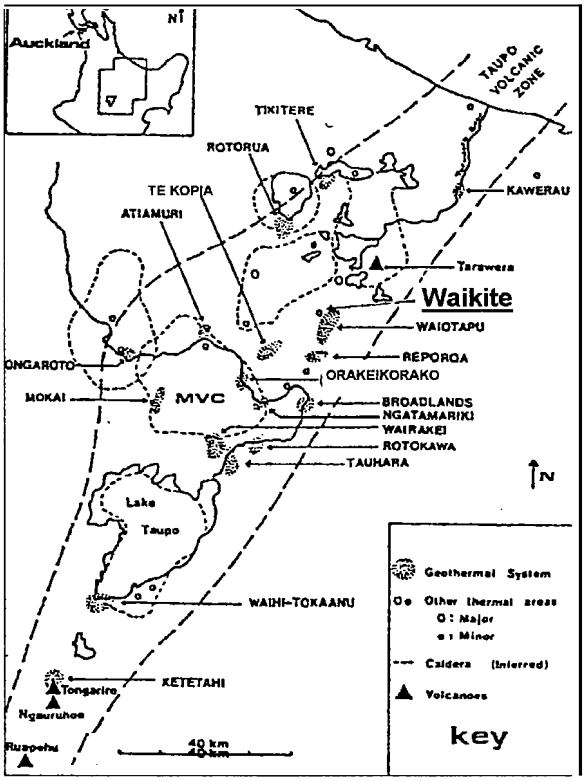

Figure 1. Location map of the Waikite area, Taupo Volcanic Zone, North Island, New Zealand (after Bignall, **1991)**

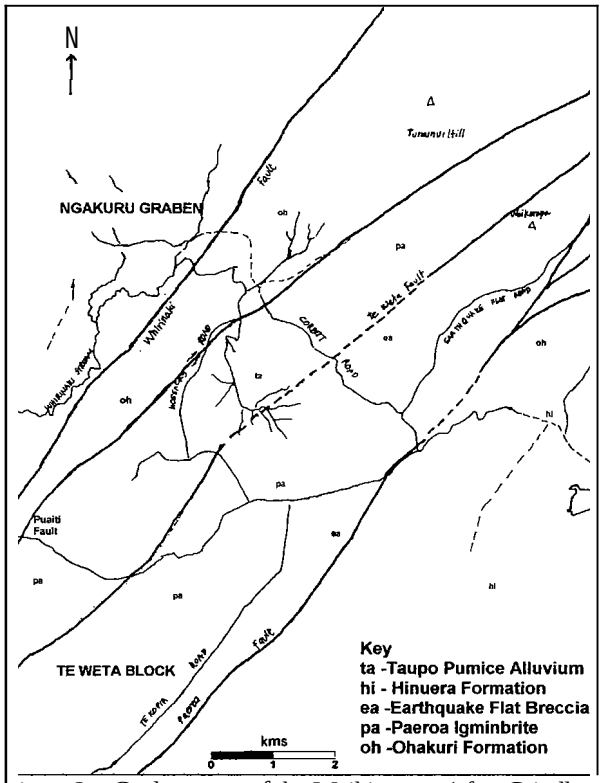

igure 2. Geology map of the Waikite area (after Grindley, **1960)**

Lying within the Te Weta block (Grindley, 1960) (Fig. 2), the Waikite area is transected by three major northeast trending faults. It is bounded on the east by the Paeroa Fault, which marks the eastern boundary. ***On*** the other hand, the Puaiti fault lies on the west and forms its western boundary. The Te Weta Fault runs in the central part of the area. Further west is the Whirinaki Fault.

Numerous workers have conducted investigations on the structure of the Taupo Volcanic Zone and numerous geophysical surveys have been carried out (von Hochstetter 1864, Grange 1937, Beck and Robertson 1955, Grange 1953, Gregg 1960, Healy et al. 1864, Lensen 1977, Walcott 1978a,b, Sissons 1979, Wan 1980, Cochrane 1983). Lensen (1958), Ridder and Lensen (1960) and Grindley (1960, 1963) used some indirect **data** and employed tectonic analysis to suggest that some northeast-trending faults are probably transcurrent or normal with horizontal displacement. Grindley (1960) assumed that the Paeroa, Te Weta and Puaiti faults may be normal-transcurrent. Cochrane and Wan (1983) showed through LANDSAT imagery the presence of major, north to northwest trending, inactive faults in the graywackes to the east of the TVZ, which may be present in the basement beneath the geothermal systems. The intersection of these faults with the younger northeast-trending faults and caldera-related structures, may be hydrologically important in providing fluid pathways and controlling the surface discharge of geothermal systems.

2.0 METHODOLOGY

2.1 Vertical Aerial Photographs

Three standard vertical aerial photographs of the Waikite **area,** with an approximate scale of 1:50,000 (SN 9445 **H/14,H/15,H/16** dtd 12/9/95), were acquired from Air Logistics (NZ) Limited. These were viewed in

stereopairs under a mirror stereoscope. Observablegeologicfeatures, such as faults and lineaments, were annotated with a pen on a transparent overlay placed on each aerial photograph (Moseley, 1981).

However, aerial photographs always have distorted scales so they cannot be used directly as maps. Distortions are usual at the edges of the aerial photos when points tend to appear to be displaced outward or inward when viewed fiom the center. These may arise because of variations in relief or may be due to the greater distance of the edge fiom the photo center (Lattman et al., 1965).

These distortions are corrected, or compensated for, by using digital image processes. First the aerial photo (middle photo was used since it covered the whole area) was converted into digital format (digitizing) by running it through a scanner. The digital image data is then fed and manipulated in a computer based digital image processing software called "Environment for Visualizing Images 3.0" (ENVI 3.0) and the output image is a rectified aerial photograph.

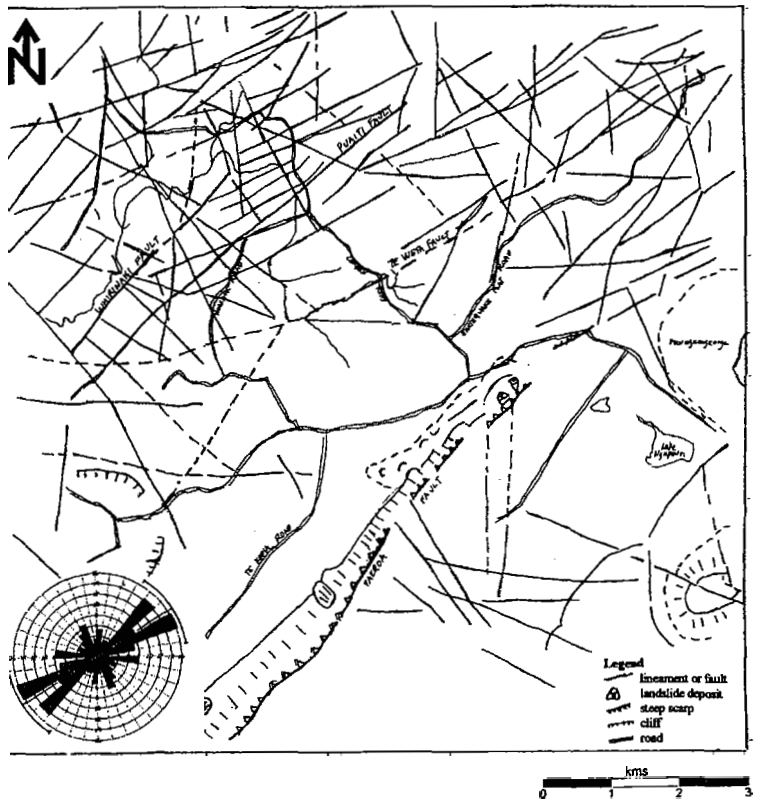

Figure 3. Lineaments from a scale-corrected aerial photograph (SN 9445,12/9/95)

The scale-corrected aerial photo was again analyzed for its geologic features in stereo pairs under a mirror stereoscope and they were annotated on a transparent overlay. The identified geological structures were compared for the two photos and with the 1:63,360 Geology Map of New Zealand Sheet N85 by Grindley. The observed lineaments, shown in Fig. 3, were plotted in rosette diagrams using computer software called Rockware 1.0.

2.2 Digital Topographic Data

Digital topographic data of the area were analyzed in the form of shaded relief maps. These data are produced fiom digitizing topographic contour maps. The DN of each pixel represents a ground resolution cell and records the average elevation of each cell (Lillesand et al., 1994). The topographic data were acquired from the Land Information Office of New Zealand. These data are stored and purchased in compact discs and come in the form of a data file (x, y and z coordinate system). These data are inputted and converted into a grid file using the computer software SURFER (version 6.03) fiom Golden Software, Inc., to produce contour or surface or shaded relief maps. The digital topographic data that were used covered an area of 40 km^2 with coordinates ffom 6310000-6318000 N and 2792000-27800000 E from the 1:50,000 NZ Grid Projection topographic map. It has a scale of 1:50,000 and elevation contour intervals at 25 meters giving it a high and smooth resolution when plotted in map form (S. Soengkono, pers comm.).

Shaded relief maps in SURFER software use different shades of a particular color to indicate the surface elevation and direction relative to a user-defined light source direction. By varying the angle of the light source, differences in relief and slope direction become emphasized.

Lineaments deduced fiom the shaded relief map were based mainly on the differences in topographical relief. These lineaments were annotated directly on the computer image or by using pencil on a printed copy of the image.

Six different light source directions or sun angles and a composite lineament map based on all other sun angles were analyzed for lineaments. The identified lineaments were plotted on rosette diagrams using a computer software called Rockware 1.0 to compare with the scale corrected aerial photo. A field inspection or "ground-truth" inspection of selected mapped lineaments from the aerial photographs and the shaded relief maps was later carried out on October 06, 1998.

3.0 RESULTS AND DISCUSSION

3.1 Lineaments Deduced from Aerial Photos

Plotted lineaments fiom the distorted aerial photo were generally displaced to the south or appeared shorter if viewed fiom the center of the photo, compared to the scale-corrected photo. The lineaments also showed no distinct trend or pattern in the rose diagram compared to the corrected photo. The succeeding discussions, therefore, refer to the scale-corrected aerial photograph shown in Fig. 3.

Five main sets of faults or lineaments were observed, based on the rose diagrams. The NE trending lineaments are most conspicuous in the aerial photos and in the field. Their preferred orientations range fiom 060" -070°, and from 040"- 070". These lineaments are long, thoroughgoing and represent the major faults traversing the area as mapped by Grindley (1960). identifiable faults in the aerial photos are the Paeroa Fault in the east, the Te Weta Fault, the Puaiti Fault and the Whirinaki Fault in the west.

The EW-trending lineaments are fewer and range fiom 2 to 3 kilometers in length. Their preferred orientations vary fiom 090"- 100". One conspicuous lineament cuts across the Paeroa and Te Weta Faults forming a linear topographic break across the ridges. The EW trending lineament in the center of the area is manifested by the alignment of the stream along its strike (6315N, 2796E). Another lineament was identified adjacent to the crater feature based on the difference in relief on both sides of the lineament (6313N, 2792E). On the eastern side of Paeroa Fault, one fault was identified based on the conspicuous depression within the thick vegetation cover (6310N, 2796E). It extends further east as a linear depression and abuts on to the caldera wall. Another EW trending fault is deduced north of this fault based on the tonal contrast on the opposite sides of the lineament (6311N, 2798E). it may represent a lithological boundary.

The NW-trending lineaments are less conspicuous in the central part of the area compared to its eastern and western extensions. Their preferred orientations vary fiom 320" to 340". Two NW trending faults are detectable across the Whirinaki stream. These are manifested as conspicuous offsets of the stream which resulted to the formation of a "zigzag" shape of the river (6317N, 2793E).

The NS-trending lineaments are few in numbers and range fiom one to two kilometers in length. Their orientation varies from 000"- 010". Most of these lineaments are made conspicuous by the differences in topographic relief, tonal contrast on opposite sides of the fault (6312N, 2792E), conspicuous alignment of the trees and the linearity of the stream channel. Other NS lineaments located north of the area, along the slope of the Tumunui Mountain, are mostly expressed as linear topographic depressions.

3.2 Digital Topographic Data

Sun Angle due East (vertical angle at 45°). Lineaments delineated at this sun angle indicate that the N-S trending lineaments are the most conspicuous set of *structures* based on the rose diagrams (Fig. 4). Their preferred orientation ranges fiom 000"- 020°. One N-S trending lineament in the west side of the area cuts across the Whirinaki, Puaiti and Te Weta faults and is almost 5 kms in length (2794-2795 E). This was not observed on the aerial photo. The Paeroa, Te Weta, Puaiti and Whirinaki faults were also identified. Their preferred orientation ranges fiom 040"- 050".

The preferred orientation of the NW-trending lineaments ranges from 310°-340". This same set of NW trending lineaments were also observed in aerial photos, however, they seem to be more conspicuous and thoroughgoing in the shaded relief map. The EW trending lineaments are few in number and as not readily observable as in the aerial photos. Their orientation ranges from 080"- 100°. It is also observed that the Waikite thermal area lies along the intersection of a northwest trending lineament and a northeast trending lineament, parallel to the Paeroa Fault.

Sun Angle due North (vertical angle ut 45°). The same set of dominant lineaments, as in the previous shaded relief map, are reflected in these rose diagrams (Fig. 5). These are the 040°-050°, 000"- 010" and the 320"-330" trending lineaments. The EW-trending lineaments are hardly evident with this sun angle. The Waikite thermal area is again seen lying along the "secondary" Paeroa Fault and a northwest trending lineament.

Sun Angle due West (vertical angle at 45°). The three conspicuous sets of lineaments are still dominant with this sun angle (Fig. 6). The NW trending lineaments appear to be more thoroughgoing (6313.5N, 2798E-6316.5N, 2796.5E) than in the aerial photographs and abut at the Paeroa scarp. The EW trending lineaments are more prominent with this sun angle than on the aerial photographs as seen in the rose diagrams. Their orientation ranges from 090"- 100".

Sun Angle due South (vertical angle at 45°). The rose diagrams still indicate the same set of dominant lineaments as in the previous shaded relief map, which are the 000°- 010°, 030"- 050" and the 310°-330" trending lineaments (Fig. 7).

Sun Angle at the Northeast (vertical angle at 35°). At this sun angle position, the most dominant set of lineaments are those trending 000"- 010" (Fig. 8). The

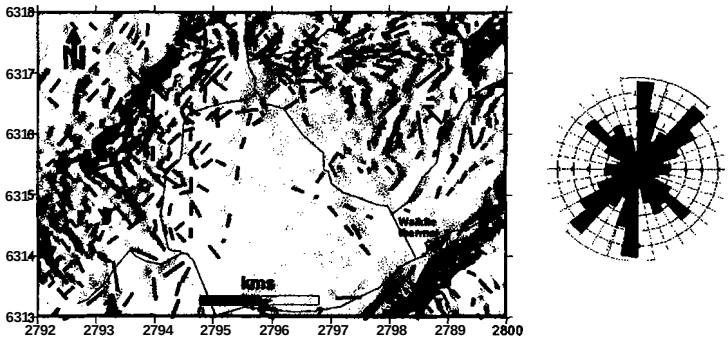

Figure 4. Lineaments inferred from the shaded relief map with the sun angle at due east and inclined at 45". Rose diagram on the right shows the orientation of dominant lineament sets.

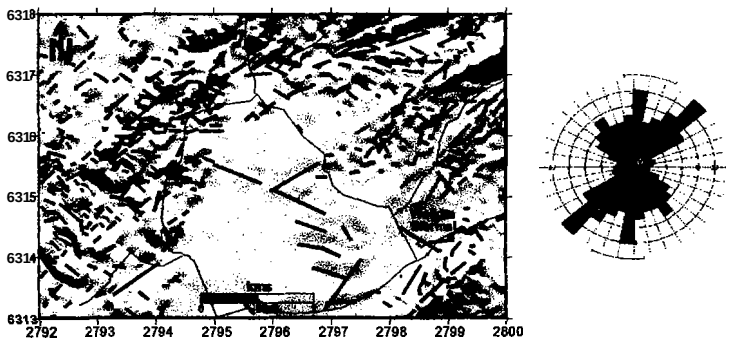

Figure 5. Lineaments inferred from the shaded relief map with the sun angle at due north and an incline of 45°.

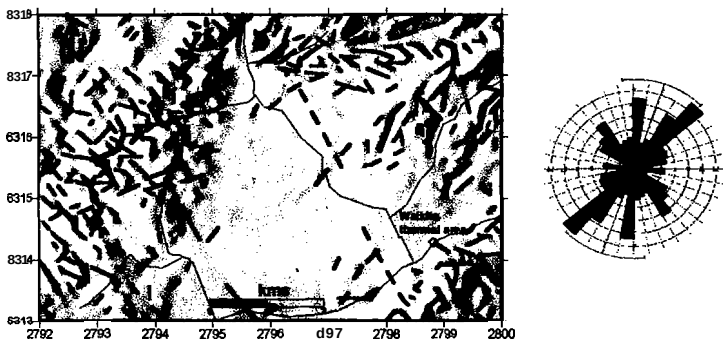

Figure 6. Lineaments inferred from the shaded relief map with the sun at due west and inclined at 45".

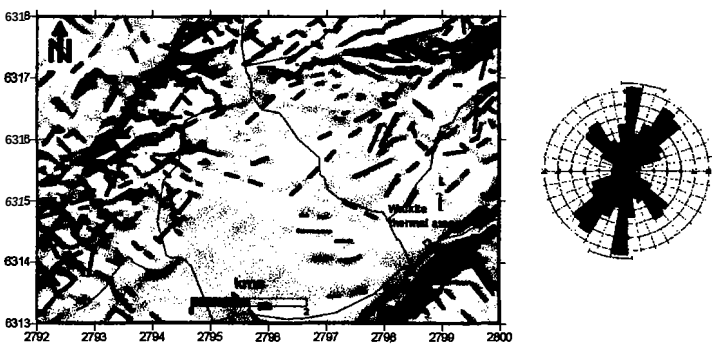

Figure 7. Lineaments inferred from the shaded relief map with the sun angle at due south and inclined at 45°.

previously identified shorter NS trending lineaments fiom aerial photos have become more conspicuous and extend further towards the south. All other lineament sets observed in the aerial photos and shaded relief map are evident but are not as conspicuous as the **NS** trending lineaments at this sun angle.

Sun Angle at the Northwest (vertical angle at 35°). Based on the rose diagram at Fig. 9, the most conspicuous set of lineaments are those trending 000"- 010°. The same set of previously identified lineaments is still observed and no new obvious lineament has been observed compared with the other sun angles.

3.3 Aerial Photographs vs. Digital Topographic Data

Based on the rose diagrams, lineaments obtained fiom the digital topographic data can be generally classified into four main sets. These are: the a) 000°- 010" trending b) **040**"- 050" trending c) **310**"- **330**" and d) 090°- 100° trending.

The orientations **of** the four fiacture sets identified fiom digital topographic data are more or less similar to those delineated on the scale-corrected aerial photographs. A second set of NE trending lineaments, with orientations ranging from **060**"- 070°, observed in the aerial photos was not as prominent in the shaded relief maps. This **is** probably because most of these lineaments had more horizontal displacements and were identified only on the basis of the alignment of vegetation, linearity of tonal contrast, the alignment **of** stream channels and stream offsets which are not discernible in the shaded relief map.

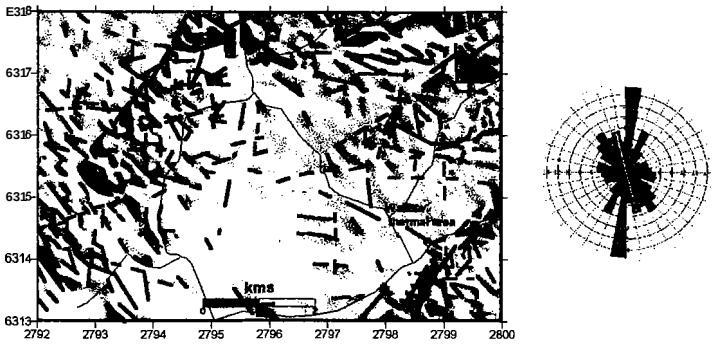

Figure 8. Lineaments inferred with the sun direction at due northeast and inclined at 35".

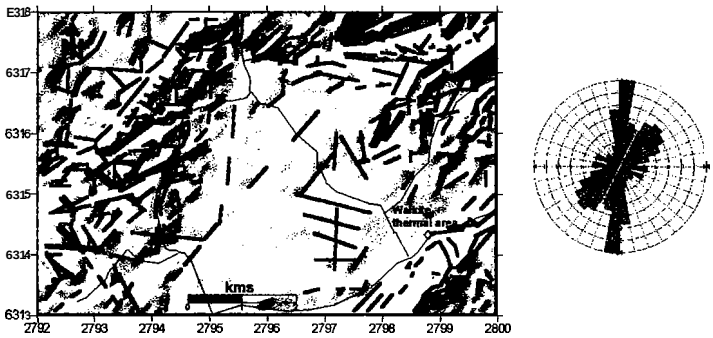

Figure 9. Lineaments inferred with the sun direction at due northwest and inclined at 35°.

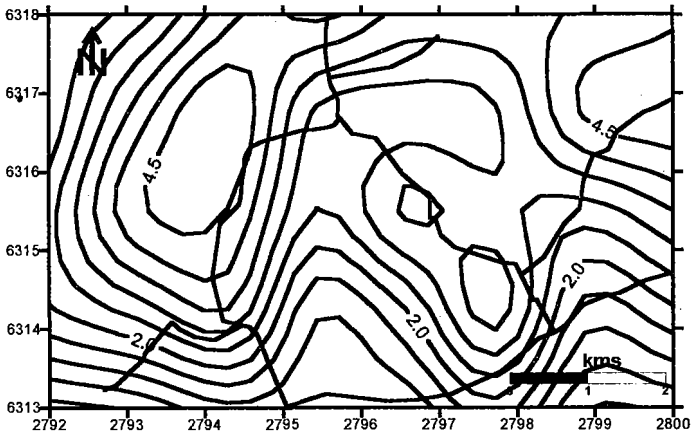

Figure 10. **A** "fault and fracture density" contour map of the Waikite area. Contour interval 0.5 km/km^2 (after Soengkono 1998, in press).

The Waikite thermal valley lies at the intersection of a northwest trending lineament and a northeast trending lineament, parallel to the Paeroa Fault. This was not evident in the aerial photographs.

A "fault and fiacture density" measurement was also employed in the analysis of the plotted lineaments (S.Soengkono, in press). This parameter measures the total length of lineaments per unit area (km/km^2). The total length **of** lineaments was summed and divided by the area of the grid (one km. grid used). Soengkono found a close correlation between a high fracture density with the location **of** the thermal area, as in Orakeikorako. The results, which are shown in Fig. 10, show a high fiacture density lobe **(4.5** km/km^2) in the northeast part of the area which

may be possibly associated with the northern group of Waikite springs called Puakohurea springs (not included in map). Another feature worth noting is the presence of a similarly high fracture density lobe, northwest of the area. This correlates with the group of hills that is the site of a fossil geothermal system (P. Browne, pers comm.).

3.4 Structural Analysis

The general orientation of the five sets of lineaments in the area from aerial photos and digital topographic data can be explained by the model of simple parallel wenching by Wilcox et al. (1973) which was simulated using clay models.

Wrench faults are formed from the movements of crustal blocks in opposite directions parallel to their adjacent edges. Parallel displacement of the blocks produce compressional and tensional stresses in the overlying rocks that can be depicted as an ellipse, as shown in Fig. 11.

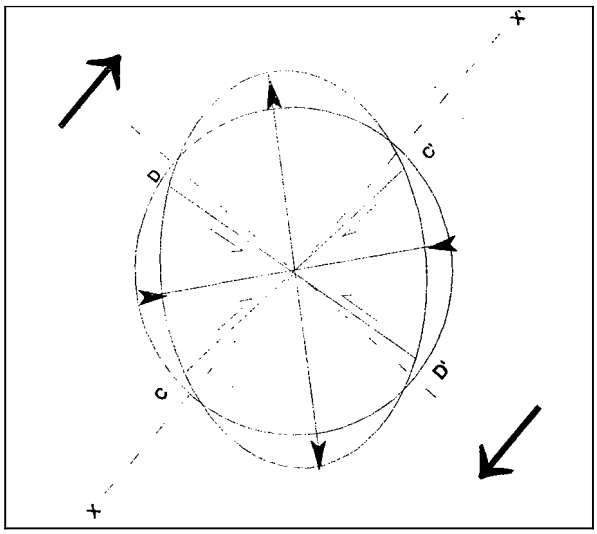

Figure 11. Strain ellipse. X-X'=wrench axis; Conjugate fracture sets C-C'= synthetic strike-slip faults, D-D'=antithetic strike-slip faults; A-A'=axis of max elongation; B-B'=axis of max compression (after Wilcox et al., 1973)

In the initial stages of wrench deformation, en echelon folds are formed at an angle always less than 45" to the main wrench strike. In most clay experiments, the angle formed between the wrench axis and the wrench strike approximates 30" ± 15" either in a clockwise or counterclockwise direction. As the amount of displacement on the wrench fault increases, these folds are broken, first by fractures then by faults. Wrenching also causes two sets of intersecting vertical fractures to form. The low angle fracture set makes an angle between 10" and 30" with the wrench strike whereas the high angle set intersects the wrench strike at an angle between 70° and 90". These conjugate fractures are either joints or faults (or both) depending upon the magnitude of the wrenching. The acute angle of intersection formed between these two conjugate fi-actures is usually in the range of 60° to 70° and depends on the nature of the rocks and the deformation. Their acute angle is bisected by the direction of maximum compression. These low angle faults have the same displacement as the main wrench fault and are called synthetic strike-slip faults. In contrast, the high angle set of conjugate strike-slip fault with a displacement sense opposite to that of the main wrench is known as antithetic strike-slip faults. As deformation continues, these conjugate fractures that have developed proceed as a combination of strike-slip faulting and plastic distortion. The acute angle between the two conjugate fractures enlarges as the two faults rotate away fkom each other. The final stage of wrench deformation is the development of the main thoroughgoing wench fault. Tension joints or normal faults may form which crosses the en echelon fold axis at right angles and bisects the acute angle of the conjugate shears. This is observed to form in the initial stages of deformation but both are easily destroyed as wrench displacement continues.

The theory used behind the clay model experiments can be applied in the Waikite area. Oblique subduction of the oceanic crust of the Pacific Plate beneath the continental *crust* of the North Island in the Tonga-Kermadec trench produce compressive forces which *can* be resolved into two components. The normal component, which is the westward subduction of the Pacific Plate, is manifested by the complex folding, faulting and uplift of the Tertiary sediments west of the TVZ. The parallel component is manifested by the dextral strike slip movements of the major faults at the North Island axial ranges and fhe Taupo Volcanic Zone. The main wrench fault in the Waikite area is represented by the Paeroa, Te Weta and Puaiti faults. Grindley (1960) and Cochrane *et* al. (1983) assumed that these faults have dextral horizontal movements. Following the assumption of these workers and the

structural pattern from the clay model, right lateral movement along the wrench strike **(040°- 050")** should produce en echelon folds oriented 010°- **015" ± 15°.** This closely resembles the 000°- 010° trending lineaments delineated **from** the digital topographic **data.** The predicted conjugate strike slip shears **(050°- 080°** and **290°-** 320") likewise approximate the delineated lineaments oriented **040°- 050"** and **320°- 330" from** the digital topographic data and aerial photographs. The 320°- 330° trending lineaments, however, are regarded by Cochrane et al. **(1983)** as basement fsults since they formed long prior to the Quaternary. This corroborates the findings from the aerial photographs since these inferred faults have a sense of displacement opposite fiom that of the model. Their right lateral movements are probably related to an older stress regime. There exists though a high possibility that they may have been reactivated during this period of deformation. The less obvious EW trending lineaments are the tensional or normal faults that form at right angles to the fold axis. So in summary, the model that best explains the lineament pattern in the Waikite area is simple parallel wrenching along the major northeast trending faults.

The Waikite thermal area, as observed in the shaded relief map, lies along the intersection of a northwest trending lineament and secondary faults of the Paeroa Fault. This is similar to Cochrane and Wan's **(1983)** findings that the geothermal fields in the TVZ lie along intersections of fault networks or the intersection of northwest inactive faults with the younger northeast trending faults.

4.0 CONCLUSIONS

Vertical aerial photo and digital topographic data were used to map and interpret geological structural features in the Waikite geothermal area. The resulting structural map was comparable to the existing geological maps of **other** workers but was more detailed. Each method was able to delineate and highlight lineaments *or* faults unique **from** each other, based on each method's degree of usefulness. These methods should be used in conjunction or should complement each other to give a detailed and comprehensive geological representation of an area.

Fault and fracture density measurements reveal two high lobes, one associated with the northernmost springs of the Waikite thermal area and the other is attributed to a fossil geothermal system located in the west of the area. The faults and lineaments in the Waikite area *can* be grouped into five main lineament sets **with** five distinct alignments. These are:

a) **040°- 050°**± 10" trending
b) **320°- 330°**± **10"** trending
c) **000°- 010"** trending
d) 090°- **100°**± 10" trending
e) 060°- 070" trending

The delineated major fracture sets in the Waikite area represent a structural deformation pattern due to simple parallel wrenching along the major northeast trending ***structures.*** **The** 060°- 070" trading lineaments **and the** 320°- 330" trending lineaments represent the Conjugate strike slip faults, the 000°- 010" trending lineaments represent the fold axis and the 090°- **100°** trending lineaments represent tensional features. Wrench faulting is associated with the oblique subduction of the Pacific Plate **beneath** the continental *crust* of the **North** Island.
The Waikite thermal area **lies** along the intersection of northeast trending **and northwest** trending lineaments fault **sets.** This supports **past** workers' findings that geothermal systems in the TVZ are located **along** these intersections.

REFERENCES

Allum, J.A.E., **1966.** Photogeology **and** Regional Mapping. Pergamon **Press,** oxford

Bibby, **RM. ,** Bennie, **S.L.,** Stagpoole, V.M., and Caldwell, **T.G.,** 1994. **Resistivity** Structure *of* the Waimangu, Waiotapu, Waikite and Reporoa Geothermal Areas, **New Zealand. Geothermics 23, 445-471.**

Bignall, G., 1994. Thermal Evolution and Fluid Mineral Rock Alteration in the Orakeikorako-Te Kopia Geothermal System, Taupo Volcanic Zone, New Zealand. Unpublished Ph.D. thesis. University of Auckland.

Bromley, C. J., 1992. Waikite-Te Kopia: The Missing Link? Proceedings 14th New Zealand Workshop, 217-222.

Cochrane, G.R. and T.F. Wan, 1983. Interpretation of structural characteristics of the Taupo Volcanic Zone, New Zealand, from LANDSAT imagery. International Journal of Remote Sensing 4, 111-128.

Cole, J.W., 1979. Structure, petrology and genesis of Cenozoic volcanism, Taupo Volcanic Zone, New Zealand- a review. NZ Journal of Geology and Geophysics. 22, 631-657.

_____ and K.B. Lewis, K.R., 1981. Evolution of the Taupo-Hikurangi Subduction System. Tectonophysics 72, 1-21.

Compton, R.R., 1962. Manual of Field Geology. J.Wiley and Sons, lnc., New York.

Ferrer, H.P., E.S. Bate, D.R. Guerrero, and A.P. Ferrer, 1981. Landsat Assisted Geostructural Analysis of the Bacon-Manito Geothermal Field, Southeastern Luzon, Philippines. Geothermal Resources Bulletin, 41-61.

Lattman, L.H. and R.G. Ray, 1965. Aerial Photographs in Field Geology. Holt, Rhinehart and Winston. New York.

Lillesand, T. M. and R.W. Keifer, 1994. Remote Sensing and Image Interpretation. 3rd edition. J. Wiley and Sons. New York.

Lueder, D.R., 1959. Aerial Photographic Interpretation, Principles and Application. McGraw-Hill Book Co., New York.

Miller, V.C., 1961. Photogeology. McGraw-Hill Book Co., New York.

Moseley, F., 1981. Methods in Field Geology. W.H. Freeman and Co., Oxford.

Sabins, F.F., 1996. Remote Sensing: Principles and Interpretation. 3rd edition. Freeman and Co., New York.

Simmons, S.F. and P.R.L. Browne, 1991. Active Geothermal Systems of the North Island New Zealand. Guide Book for North Island Field Tour. Geological Society of New Zealand Misc. publication 57.

Stewart, M.K., 1994. Groundwater Contributions to Waikite Geothermal Fluids. Proceedings 16''NZ Geothermal Workshop, 109-114.

Sylvester, A.A. Wrench Fault Tectonics. Selected papers reprinted from the AAPG Bulletin and other geological journals. AAPG Reprint Series 28.

Wilson, C.J.N., B.F. Houghton, M.O. McWilliams, M.A. Lamphere, S.D. Weaver, and R.M. Briggs, 1995. Volcanic and Structural Evolution of Taupo Volcanic Zone, New Zealand a review. Journal of Volcanology and Geothermal Research 68, 1-28.